The vertical occipital fasciculus: A century of controversy resolved by in vivo measurements

Jason D. Yeatman[a,b,c,1,2], Kevin S. Weiner[a,b,1,2], Franco Pestilli[a,b], Ariel Rokem[a,b], Aviv Mezer[a,b], and Brian A. Wandell[a,b,2]

[a]Department of Psychology and [b]Center for Cognitive and Neurobiological Imaging, Stanford University, Stanford, CA 94305; and [c]Institute for Learning and Brain Sciences, University of Washington, Seattle, WA 98195

Contributed by Brian A. Wandell, October 14, 2014 (sent for review May 2, 2014; reviewed by Charles Gross, Jon H. Kaas, and Karl Zilles)

The vertical occipital fasciculus (VOF) is the only major fiber bundle connecting dorsolateral and ventrolateral visual cortex. Only a handful of studies have examined the anatomy of the VOF or its role in cognition in the living human brain. Here, we trace the contentious history of the VOF, beginning with its original discovery in monkey by Wernicke (1881) and in human by Obersteiner (1888), to its disappearance from the literature, and recent reemergence a century later. We introduce an algorithm to identify the VOF in vivo using diffusion-weighted imaging and tractography, and show that the VOF can be found in every hemisphere ($n = 74$). Quantitative T1 measurements demonstrate that tissue properties, such as myelination, in the VOF differ from neighboring white-matter tracts. The terminations of the VOF are in consistent positions relative to cortical folding patterns in the dorsal and ventral visual streams. Recent findings demonstrate that these same anatomical locations also mark cytoarchitectonic and functional transitions in dorsal and ventral visual cortex. We conclude that the VOF is likely to serve a unique role in the communication of signals between regions on the ventral surface that are important for the perception of visual categories (e.g., words, faces, bodies, etc.) and regions on the dorsal surface involved in the control of eye movements, attention, and motion perception.

diffusion-weighted imaging | vertical occipital fasciculus | perpendicular fasciculus | quantitative T1

The vertical occipital fasciculus (VOF) is the only major fiber bundle connecting dorsal and ventral regions of occipital, parietal, and temporal cortex. The signals carried by the VOF are likely to play an essential role in an array of visual and cognitive functions. Characterizing the VOF connections and tissue structure in the living human brain is important for the study of human vision and cognitive neuroscience alike.

Carl Wernicke discovered the VOF (1). For the next 30 y, the VOF was included in many major neuroanatomy atlases and journal articles (1–14). However, Wernicke's study contradicted a widely accepted principle of white-matter organization proposed by Meynert, Wernicke's mentor. Over the subsequent decades, there emerged a camp of neuroanatomists who acknowledged Wernicke's discovery and another group that, like Meynert, disregarded the discovery. Due to its controversial beginnings, haphazard naming convention, and the difficulty of standardizing postmortem procedures, the VOF largely disappeared from the literature for most of the next century. A century later, Yeatman et al. (15) rediscovered the VOF using diffusion magnetic resonance imaging (dMRI); they were the first to characterize the VOF cortical projections in the living, behaving, human brain.

Why would such an important pathway disappear from the literature for so long? The disappearance can be traced to controversies and confusions among some of the most prominent neuroanatomists of the 19th century (1–13, 16–18). Modern, in vivo, MRI measurements and algorithms allow for precise, reproducible, scalable computations that can resolve these century-old debates and provide novel insight into the architecture of the VOF in the living human brain.

This article is divided into five sections. First, we review the history of the VOF from its discovery in the late 1800s (1) through the early 1900s. Second, we link the historical images of the VOF to the first identification of the VOF in vivo (15). Third, we describe an open-source algorithm that uses dMRI data and fiber tractography to automate labeling of the VOF in human (github.com/jyeatman/AFQ/tree/master/vof). Fourth, we quantify the location and cortical projections of the VOF with respect to macroanatomical landmarks in ventral (VOT) and lateral (LOT) occipito-temporal cortices. Fifth, we report in vivo histological measurements, using quantitative T1 mapping, which differentiate VOF tissue properties from surrounding pathways. We conclude by discussing how computational neuroanatomy improves the clarity of tract definition and reproducibility of anatomical results.

The History of the VOF

We describe the history of the VOF, beginning with its discovery in the late 19th century, the contentious debate that followed its discovery, and how modern MRI techniques resolved the debate. We use the name "vertical occipital fasciculus" throughout even though others refer to this pathway with various names (Table 1).

Student vs. Mentor I: Wernicke's Discovery of the VOF in Monkey Contradicted Meynert's Theory of Association Fibers

Theodor Meynert was a German–Austrian neuroanatomist whose many prominent students included Wernicke, Korsakoff, and Freud. As director of the psychiatric clinic in the University of Vienna, Meynert used neuroanatomy to understand the basis of mental illness; he established the study of cytoarchitectonics and

Significance

The vertical occipital fasciculus (VOF) is a major white-matter fascicle connecting dorsal and ventral visual cortex. Few vision scientists or cognitive neuroscientists are aware of the VOF's existence. The scarcity of papers on this important pathway stems from the contentious history surrounding its discovery by Wernicke in 1881. We review the conflict surrounding the classic, postmortem, VOF measurements, and we introduce modern, in vivo methods to precisely characterize the VOF's cortical terminations and unique tissue properties. The new VOF measurements provide insight into the communication between ventral stream regions involved in form perception and dorsal stream regions involved in eye movements and attention.

Author contributions: J.D.Y., K.S.W., and B.A.W. designed research; J.D.Y. and K.S.W. performed research; J.D.Y., K.S.W., F.P., A.R., A.M., and B.A.W. contributed new reagents/analytic tools; J.D.Y., K.S.W., F.P., A.R., and A.M. analyzed data; and J.D.Y., K.S.W., and B.A.W. wrote the paper.

Reviewers: C.G., Princeton University; J.H.K., Vanderbilt University; and K.Z., Research Center Juelich.

The authors declare no conflict of interest.

[1]J.D.Y. and K.S.W. contributed equally to this work.

[2]To whom correspondence may be addressed. Email: wandell@stanford.edu, jdyeatman@gmail.com, or kweiner@stanford.edu.

Table 1. The many names and abbreviations of the VOF

Author (year)	Name (abbreviation)	Species	Reference to the discovery
Wernicke (1881)	Senkrechte Occipitalbündel (*fp*)	Macaque (likely)	
Edinger (1885, 1896, 1904)	—	Human	Wernicke (not until 1896)
Obersteiner (1888)	Senkrechte Occipitalbündel (*fov*); fasciculus occipitalis perpendicularis (*Op*)	Human	Wernicke
Schnopfhagen (1891)	Senkrechte Occipitalbündel (*d*, *d′*)	Calf embryo	Contests Wernicke
Sachs (1892)	Stratum profundum convexitatis	Human	Homologous to fasciculus occipitals perpendicularis of Wernicke
Quain's Anatomy (1893)	Perpendicular fasciculus (*fp*)	Human	Wernicke, Sachs
Vialet (1893)	Faiceau perpendiculaire de la convexité	Human	Wernicke
Dejerine (1895)	Faisceau occipital vertical (*Ov*); Faisceau perpendiculaire de la convexité	Human	Wernicke, Sachs
Barker (1899)	Fasciculus occipitalis verticalis, or perpendicularis, of Wernicke (*Ov*)	Human	Wernicke, Sachs
Jakob and Fisher (1901)	Fasciculus rectus	Human	—
Vogt (1904)	Stratum posterius subcorticale ($it + it^1 + sc$)	Human	Wernicke, Sachs
Von Monakow (1905)	Fasciculus occip. Verticalis; verticalen Occipitalbündel	Human	Contests Wernicke
Archambault (1909)	Vertical occipital fasciculus	Human	Wernicke
Curran (1909)	Fasciculus transversus occipitalis (*F. trans. o.*, *F. trans. o.*^{1}, *F. trans. o.*^{2})	Human	—
Herrick (1918)	Fasciculus transversus occipitalis (*f. tr. occ.)*	Human	—
Kuhlenbeck (1927)	Fasciculus transversus occipitalis (*to*)	Human	—
Bailey et al. (1943)	Vertical occipital fasciculus	Human, chimpanzee	Wernicke

myeloarchitectonics in the postmortem human brain (19). Meynert's work greatly influenced Flechsig, Brodmann, and others who went on to pioneer important insights into myelinogenesis and cytoarchitectonic organization of the cerebral cortex.

Meynert used the term "fibrae propriae" (20, 21) to describe the association fibers connecting different cortical regions within a hemisphere. He classified these fibers into two categories, short and long. The short U-shaped fibers connected different sides of a gyrus, and the long fiber bundles connected widely separated cortical regions within each hemisphere. Meynert claimed that the long association fibers were all anterior-posterior, and he viewed the orientation of the long fibers as a general principle of brain anatomy. In 1872, Meynert published a landmark article explaining these principles that would define how other neuroanatomists of the era would classify the brain's fiber systems. French neurologist Jean-Martin Charcot (who also trained Sigmund Freud, Ludwig Edinger, and Bernard Sachs—translator of Meynert's *Psychiatrie*) described Meynert's association fiber principle:

> [Association fiber bundles] are composed of fibres having, as a rule, an antero-posterior direction, which bring into relation different parts of the same hemisphere. The accompanying figure, borrowed from Meynert, and representing the anterior section of a monkey's cerebrum (Cercocebus cinomolgus), shows well the direction of the principal fasciculi of this antero-posterior association system (ref. 22, pp. 111–112).

Meynert retained this theory of association fibers and their general antero-posterior trajectory until his death (1892) when his final paper was published on association bundles in the human brain (Fig. 1*B*).

In the late 1870s and early 1880s, Heinrich Neumann sent his student, Carl Wernicke, to work in Meynert's laboratory to study neuroanatomy. The stay was short (about 6 mo), but it greatly shaped Wernicke's understanding, and he went on to pioneer the emerging fields of cytoarchitectonics and connectionism in human and animal models (23).

In monkey, Wernicke described a long association fiber bundle in the posterior occipital lobe that defied Meynert's principle of long anterior-posterior association bundles (1). (Wernicke does not specify the species. However, in their 1951 atlas, Von Bonin and Bailey speculate it was macaque.) Instead, Wernicke's "senkrechte Occipitalbündel," or vertical occipital bundle, was oriented vertically, perpendicular to the longitudinal plane of the other long association fibers. Wernicke asserted that these fibers extended from the angular gyrus dorsally to the fusiform gyrus ventrally (Table 1 and Fig. 2). In his 1881 atlas, he writes the following:

> On sagittal slices of the monkey brain there also appears an only recently found, but also massive, set of association fibers, which connects the upper tip of the angular gyrus with the fusiform gyrus, i.e., the vertical occipital bundle (ref. 1, p. 23).[†]

Student vs. Mentor II: Obersteiner's Discovery of the VOF in Human Is Incorporated into Major Neuroanatomical Atlases

Heinrich Obersteiner, founder of Vienna's Neurological Institute and another student of Meynert, was the first to identify a homologous vertical association fiber in human (2) (Table 1 and Fig. 2). Obersteiner's discovery was overlooked, perhaps because it was one observation in a very long (several-hundred page) atlas that covered the entire nervous system. In 1892, Heinrich Sachs provided simple and clear images of this vertical bundle in a much shorter atlas focused on white matter. Also, Sachs included evidence for the fascicle in the form of stained coronal sections rather than relying on camera lucida drawings. Consequently, Sachs, a student of Wernicke, is typically credited with the discovery of the human VOF (Table 1, right column).

In this fertile period of human neuroanatomy, many structures were discovered (24–29). During this discovery phase, each neuroanatomist developed their own nomenclature. For example, Wernicke, Obersteiner, and Sachs all identified what they believed to be the same pathway, but each used a different name (Table 1). In each of the four figures included in Wernicke's 1881 atlas, Wernicke refers to the VOF as *fp* (Fig. 1), which then triggered the eponyms of this pathway as "Wernicke's perpendicular fasciculus" or "perpendicular occipital fasciculus of Wernicke" (30, 31). Within a single atlas, Obersteiner used two different abbreviations for the VOF in two figures (Figs. 2 and 3)

[†]"Auf Sagittalsschnitten durch das Affengehirn tritt noch ein erst neuerdings gefundenes*), ebenfalls mächtiges Associationsbündel hervor, welches die oberste Spitze des unteren Scheitellappchens mit der Spindelwindung verbindet, das senkrechte Occipitalbündel" (p. 23).

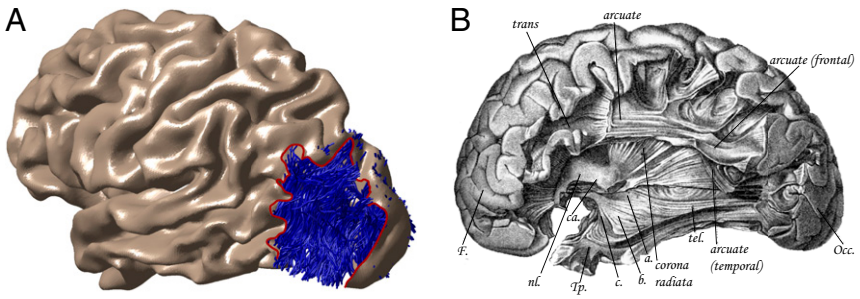

Fig. 1. Meynert's association fiber system excluded the VOF. (*A*) The surface of the lateral occipital lobe has been removed (dotted line) to show the location of the VOF for a representative subject. The individual's cortical surface was reconstructed from a segmented T1-weighted image, and the VOF was identified in vivo with diffusion-weighted imaging (see *Methods*). (*B*) By the late 1800s, Myenert had described most of the brain's major white-matter fascicles but did not acknowledge the existence of the VOF. Meynert differentiated short (U-shaped fibers) and long (arcuate, inferior longitudinal, uncinate, and cingulate fasciculi) association fibers. He believed long association fibers connected anterior and posterior regions within each hemisphere, and he did not acknowledge the dorsal-ventral VOF. Even in his last paper—11 y after Wernicke described the VOF—Meynert omitted the dorsal-ventral VOF from published images. The figure labels the major anterior-posterior tracts, but the occipital cortex remains in place, covering the position of the VOF [figure 3 from Meynert (1892) (34) published in the year of his death].

as the *fov* and *Op*. Sachs referred to the VOF as "stratum profundum convexitatis" (Fig. 2 and Table 1). We suspect that this haphazard naming convention contributed to the disappearance of the VOF from the literature.

Wernicke, Obersteiner, and Sachs, as well as other authors of that era place the VOF 2–3 cm anterior to the occipital pole (Fig. 3). The consistency of the observation can be overlooked because of the inconsistency of the terminology. In 1893, Sir Edward Schaefer incorporated a modified version of Obersteiner's schematic into one of the most widely used anatomical atlases of the time, *Quain's Anatomy* (5). Obersteiner's atlas also was widely used and translated into four different languages, so that the VOF was extensively documented by the early 1890s. Variations of this schematic were later used in other influential atlases such as *Gray's Anatomy* (Fig. 3) and the schematic was directly reproduced in a mid-20th century journal article comparing the location of the VOF in monkeys and chimpanzees using strychnine neuronography (17) (Table 1) and later referenced in an accompanying atlas (32).

Contesting the VOF: Unimportant and Hard to Find

Although there were early, consistent descriptions of the VOF, its existence became contentious and many neuroanatomists disregarded the pathway. We speculate these disagreements contributed to the omission of the VOF over the next 100 y.

Meynert, even at the time of his death in 1892 and a decade after Wernicke's discovery, did not accept the VOF. Indeed, in his final article, Meynert clarified the organization of the other association bundles that had been discovered, but omitted any reference to the VOF (Fig. 1*B*). This omission might reflect the fact that the VOF's vertical trajectory violated Meynert's principle that long association tracts run anterior-posterior. Meynert was known for supporting his students (33), and his refusal to acknowledge Wernicke's discovery of the VOF is surprising. Edinger's influential atlas and lecture series adopted Meynert's view; this probably influenced a prominent group who all failed to include the VOF in their descriptions (Fig. 3, "Edinger, 1885").[‡]

Another major group of scientists specifically argued against the existence of the pathway. Schnopfhagen was the first to directly challenge the existence of the VOF (3), arguing that it was nothing more than an interlacing field of fibers on the convexity of the lateral surface extending from the inferior longitudinal fasciculus (ILF). In two paragraphs of his 1892 atlas, Sachs defended the VOF against Schnopfhagen's interpretation. Sachs did not mention that Schnopfhagen's arguments were based on measurements from calf embryos.

Constantin Von Monakow, the eminent Russian–Swiss neurologist, also argued against the existence of the VOF. In his 1905 atlas of the human brain, Von Monakow specifically questioned the definition of several association fibers as distinct fascicles, including Wernicke's vertical Occipitalbündel, the fasciculus transversus lobi lingualis of Vialet, and the stratum transversum cunei of Sachs (11). In his very rough drawings, Von Monakow accurately depicts the location of the VOF and yet relabels these fibers as "großes retroventrikuläres Markfeld." Von Monakow writes the following:

> In the frontal slices through the occipital white matter, just anterior to the beginning of the posterior horn (or cornu) of the lateral ventricle and anterior to the differentiation of the sagittal bundles (2–3 cm away from the occipital pole), one sees, in the white matter region that I named 'large retroventricular white matter area', a sizable amount of fibers that run through the entire matter both horizontally and vertically; but here as well it is not possible to recognize further anatomically differentiated sets of association fibers (ref. 11, p. 72).

Other authors also doubted the VOF (8). However, Von Monakow's interpretation of his data were disputed in a 1909 case study. La Salle Archambault compares a case of cerebral softening to Von Monakow's reports (12). Archambault claimed that Von Monakow's findings actually provide proof of the VOF:

> It is well to recall, in this connection, that von Monakow is among those who regard the external sagittal layer as an association tract, and it may further be stated, that the same author does not recognize the existence of Wernicke's vertical occipital fasciculus. This combination of factors largely suffices to explain von Monakow's interpretation of the degenerative picture in his case. It seems to me, however, that he has by this very instance furnished a most convincing demonstration of the existence of Wernicke's bundle (ref. 12, p. 127).

Alfred Campbell went beyond anatomy to question the functional significance of the VOF (10). In his highly influential cytoarchitectonic analysis of the brain, Campbell discusses the significance of several pathways. He dismisses the importance of the VOF:

> The fasciculus occipitalis verticalis or perpendicularis of Wernicke—stratum proprium convexitatis of Sachs—lies beneath the cortex on the lateral surface of the lobe, and is said to unite the gyri above with

[‡]In the year following Meynert's death, Edinger edited his original schematic to include fibers that looked like the VOF; he still did not label them. In the 1896 and subsequent editions, he acknowledged Sachs, Wernicke, and Vialet for discovering association pathways. Still, he did not reference the VOF. Perhaps this was out of respect for Meynert, who visited Edinger's laboratory in the late 1880s to congratulate him on the discovery of what we now know as the Edinger–Westphal nucleus.

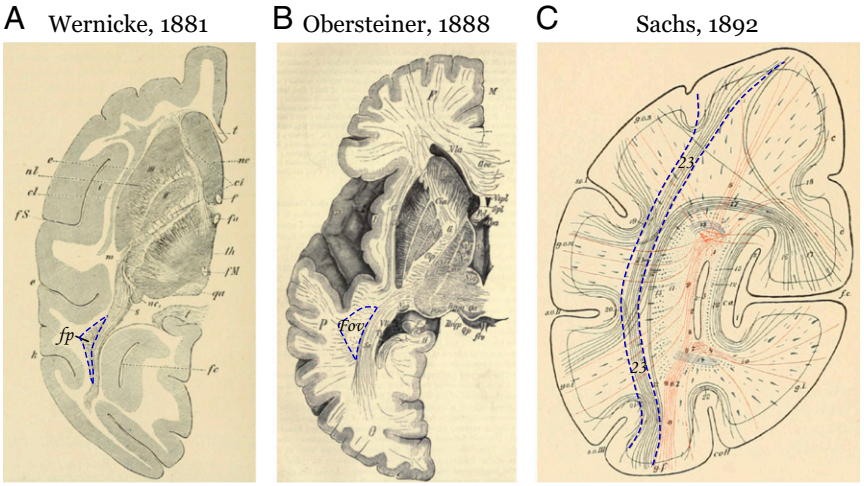

Fig. 2. The first images of the VOF in monkeys and humans. The authors referred to the VOF using different names and abbreviations. The dashed blue line highlights the location marked as the VOF by each author. (*A*) Semischematic axial slice from a monkey brain in the original identification of the VOF [figure 19 from Wernicke (1881) (1)]. *fp*, senkrechtes Occipitalbündel (VOF); *k*, vordere Occipitalfurche. (*B*) Semischematic axial slice from a human brain [figure 21 from Obersteiner (1888) (2)]. *fov*, fasciculus occipitalis verticalis of Wernicke. (*C*) Schematic coronal slice from a human brain [figure 3 from Sachs (1892) (4)]. Pathway 23: stratum profundum convexitatis (VOF).

those below, but as a matter of fact the definition of this band is difficult, and we cannot attach much importance to it (ref. 10, p. 142).

Imprecise Methods Are Blamed for Propagating Confusion About the VOF

Contrary to these contentions, and in the same year of Archambault's argument with Von Monakow over the existence of the VOF, three journal articles described dissection methods for accurate localization of white-matter pathways. Jamieson (1909) clearly states the motivation to move away from schematics and single histological slices in textbooks and atlases to depictions of dissections for accurate localization across research groups. Jamieson (1909) writes the following (35):

> Dissections of the brain to show the internal structure, as contrasted with slicing, is not a new method, but the practice has fallen into disuse, and apparently even into dishonour. Illustrations of the internal structure of the brain in the current text-books of anatomy and of physiology are almost all drawings of sections, or they are merely schemata. A few dissections are still reproduced from the old text-books (ref. 36, p. 226).

Shortly thereafter, Hoeve (1909) clearly described how to identify many white-matter pathways including the VOF (36):

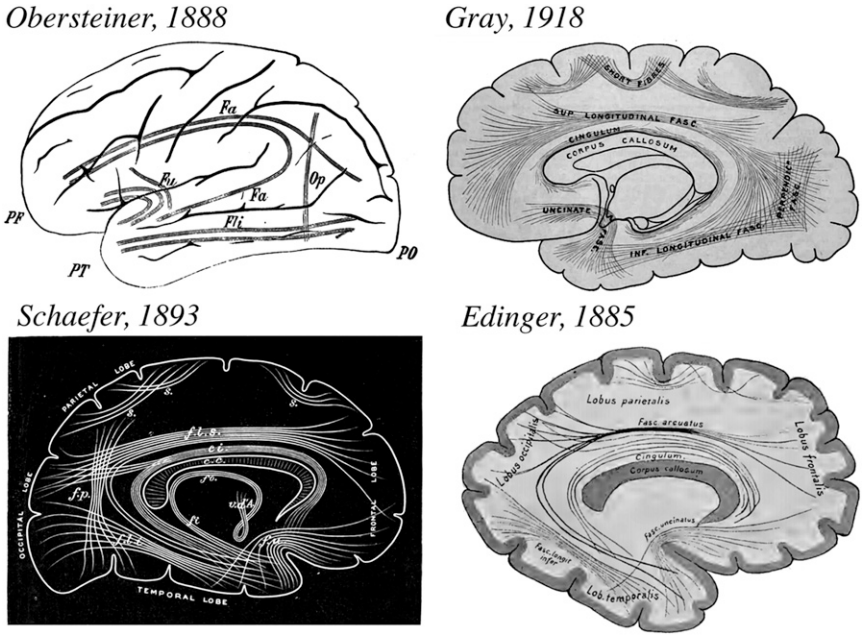

Fig. 3. Schematics of the association fibers. Several schematics include the VOF as a major dorsal-ventral connection in the occipital lobe (Obersteiner, Gray, Schaefer). These researchers consistently illustrated white-matter fibers connecting dorsal and ventral portions of the occipital lobe ~2–3 cm anterior to the occipital pole. Following Meynert, many prominent scientists, including Edinger (90), omitted the VOF from the list of association fibers. Note that Edinger's schematic (91) labels the major anterior-posterior fibers but does not include the VOF. In subsequent atlases, Edinger did not label the VOF.

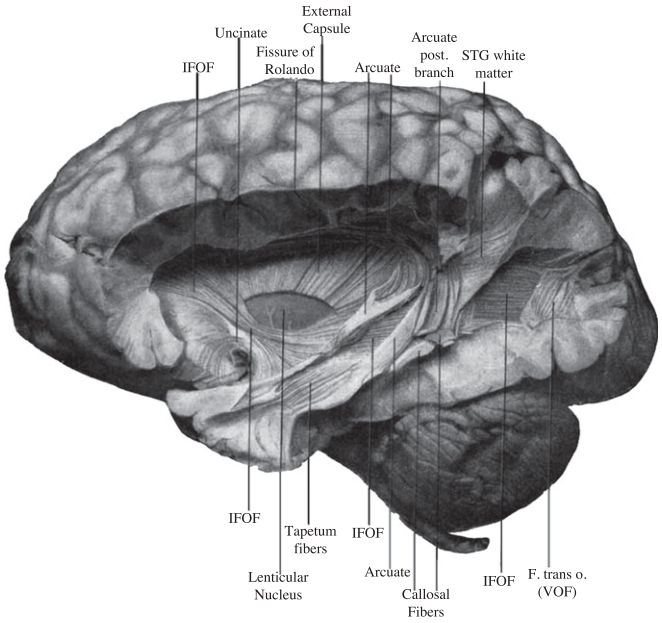

Fig. 4. The VOF in the postmortem human brain. A postmortem dissection of the VOF, reproduced from figure 1 in Curran (1909) (14), which he labeled the transverse occipital fasciculus (F. trans o.). The VOF label is added to the image. The VOF is posterior to the arcuate fasciculus and lateral to both the inferior longitudinal fasciculus (ILF) and the inferior frontal occipital fasciculus (IFOF).

> *Fasc. Perpendicularis (Wernicke).* Break the gyri of the external surface of the lobus occipitalis and find perpendicular fibres, three-fourths inch internal to its external surface and one inch anterior to the polus occiptalis (ref. 37, pp. 249–250).

Curran (1909) documents the VOF with such precision and clarity that one might have expected his work to be regarded as a resolution to the controversy (14). Referring to the VOF under a new name, the transverse occipital fasciculus (Table 1), he writes the following:

> The fasc. trans. occ. is very striking in its appearance, size, and complete isolation from the longitudinal fibers under it, among which is the fasciculus occipito-frontalis inferior. It is easily dissected as a broad vertical bundle about half an inch in depth and extending in width from the pole of the occipital lobe to the arcuate fibers (ref. 14, p. 656).

However, Curran's VOF work is usually overlooked due to a controversy surrounding another pathway, the inferior frontal occipital fasciculus (IFOF) (37). In the century following Curran's publication, few scientists had the opportunity to appreciate the exquisite images he published of the VOF and its neighboring fascicles (Fig. 4).

Given this confusion and controversy around the VOF, combined with its many (and inconsistent) names (Table 1), the pathway is now seldom mentioned in the literature. The postmortem methods available at the turn of the century relied on the eye of the scientist and observations were difficult to standardize across laboratories—only Curran and Hoeve provided a clear way to discriminate the VOF from neighboring white matter. Their approach was not widely adopted. Nearly a century passed until measurement techniques became available for precise, reproducible, definitions of white-matter fascicles.

A Modern Resolution: The VOF Exists and Is Functionally Relevant

The VOF returned to the literature with the publication of two case studies connecting the VOF with a specific cognitive function (29, 30). Greenblatt (1973) described a patient with a tumor that severely damaged posterior white matter, including the VOF; the patient developed pure alexia (38). Greenblatt (1976) subsequently described a patient with a surgical resection of the VOF; the patient also developed pure alexia (39). With the tools available at the time, there was no opportunity to specifically localize the VOF. However, in both cases, the damage was most pronounced in VOT white matter, and specifically included the anterior portion of the VOF. From these case studies, Greenblatt made a compelling argument that the VOF carries important information for reading.

Yeatman et al. (15) were the first to identify the VOF in the living human brain and to describe its cortical terminations with respect to functionally defined regions in VOT cortex (Fig. 5). These in vivo dMRI measurements make it possible to measure fMRI responses at the VOF termination points in the behaving human brain. Yeatman et al. write that the VOF:

> Ascends from the OTS, immediately lateral to ILF fibers, before branching laterally toward its cortical endpoints in the lateral occipital and inferior parietal lobes. This tract appears to connect VOT cortex to the lateral occipital parietal junction, including the posterior angular gyrus and lateral superior occipital lobe (ref. 5, pp. 6–7).

The VOF could be clearly identified in each brain as a cluster of voxels containing vertically oriented fibers immediately lateral to the inferior longitudinal fasciculus (Fig. 5). Yeatman et al.

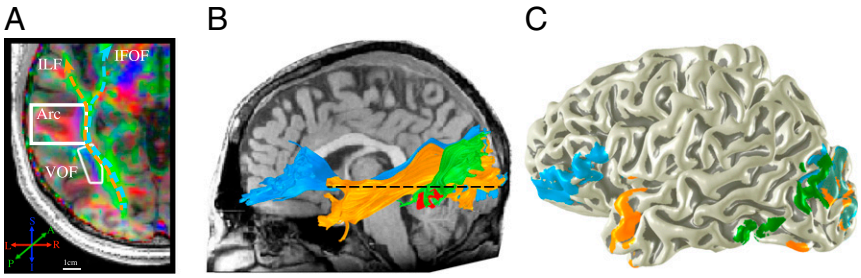

Fig. 5. The VOF in the living human brain. (*A*) The core of the VOF can be clearly identified in each brain as a cluster of voxels lateral to the ILF with a vertically oriented principal diffusion direction (PDD). The axial slice through the core of the VOF shows each voxel color-coded based on its PDD (blue, vertical; green, longitudinal; red, medial/lateral). (*B*) The VOF (green) and adjacent ILF (orange) and IFOF (blue) tracked in an individual subject based on diffusion-tensor deterministic tractography. The dashed line shows the location of the slice in *A*. The ventral terminations of the VOF are immediately adjacent to the visual word form area (VWFA) (red surface). (*C*) VOF endpoints projected to an individual's cortical surface. Newer data acquisitions and tractography methods that model multiple fiber populations in each voxel show that VOF projections are much more extensive than can be seen in either a postmortem dissection or tensor model-based visualization of diffusion-weighted imaging data. However, the core of the tract can be clearly visualized with a tensor model, and with as few as six diffusion directions and a *b* value of 1,000.

suggested that the visual word form area (VWFA), a region in the occipital temporal sulcus that plays a crucial role in skilled reading, is located at the anterior ventral terminations of the VOF.

As the VOF literature evolves, some of the historical disputes about the location and function of the pathway remain (40–42). Recent advances in dMRI, fiber tractography, and quantitative MR techniques, make it possible to eliminate the confusion. In the following section, we describe computational methods that reliably identify the trajectory, cortical connections, and biological properties of the VOF in the living human brain.

Results

A Modern Picture of VOF Anatomy and Function. Advances in noninvasive, in vivo, brain measurement techniques make it possible to precisely map the cortical circuits that are connected by the VOF and to draw inferences about the nature of the signals that are carried by this pathway. In the following sections, we introduce an algorithm to identify the VOF in individual brains with diffusion-weighted imaging and fiber tractography. We then apply this algorithm to comprehensively map the VOF's cortical projections with respect to macroanatomical landmarks. Finally, we measure the unique properties of the tissue composing the VOF in relation to neighboring occipital lobe fascicles.

A Tractography Algorithm to Reproducibly Define the VOF from dMRI. Anatomists at the turn of the century were aware that the VOF is smaller than other major association bundles, and that it passes through a complex region of crossing fibers. These two properties made it difficult to see in the postmortem brain and also made it hard to define from early dMRI techniques. For example, Yeatman et al. (2012) underestimated the posterior extent of the VOF that intermingles with the ILF, IFOF, and optic radiation.

The major neuroanatomists agreed that the ventral terminations of the VOF are in the fusiform, inferior occipital, or inferior temporal gyri. However, there was uncertainty as to the anterior boundary of the pathway and whether dorsal VOF projections were confined to the occipital lobe or spread into the parietal lobe as well. Here, we describe an algorithm that incorporates the anatomical observations to estimate the full-extent of the VOF from T1-weighted and dMRI data (Fig. 6; open-source MATLAB code; github.com/jyeatman/AFQ/tree/master/vof).

Identify ventral occipital temporal cortex (VOT), including the fusiform, inferior occipital, and inferior temporal gyri, from a segmentation of a T1-weighted image (see *Methods*). Calculate a whole-brain connectome from the dMRI data. Each fiber that terminates in VOT is included in a candidate set of fibers for the VOF. A conservative selection process for the VOF is to (*i*) retain the candidate fibers that are primarily vertical for most of their length, and (*ii*) remove fibers that intermingle with the arcuate fasciculus. This algorithm produces a conservative estimate of the anterior-posterior extent of the VOF without imposing constraints on the dorsal endpoints.

The dMRI-Defined VOF. At the time Wernicke discovered the VOF, neuroanatomists had not adopted a consistent labeling scheme of the human gyri and sulci. Consider that Wernicke defined the VOF as a white-matter fiber bundle extending between the fusiform and angular gyri. It is important to recognize that his definition of these gyri differed from his contemporaries and modern definitions. Wernicke defined the fusiform as extending to the superior temporal sulcus; he defined the angular gyrus as extending to the occipital lobe (Fig. 2, the anterior occipital sulcus labeled as k) (1, 43). Many prominent neuroanatomists, including Cunningham, Smith, and Eberstaller, rejected Wernicke's definitions (44–46). The absence of standards made it difficult to compare results across laboratories, and these disputes echo in the modern literature (40–42, 47).

Recently, the macroanatomy of human VOT (48, 49) and LOT cortex extending into the parietal lobe (50) has been clearly delineated. We use these modern definitions of gyri and sulci in human VOT and LOT to quantify the locations of the VOF cortical terminations in a large sample of human brains ($n = 37$).

The VOF can be identified automatically from diffusion measurements in every hemisphere we have measured ($n = 74$). The VOF occupies a stereotypical location, posterior to the arcuate fasciculus, as well as lateral to the inferior longitudinal fasciculus and the inferior frontal occipital fasciculus, extending ~1

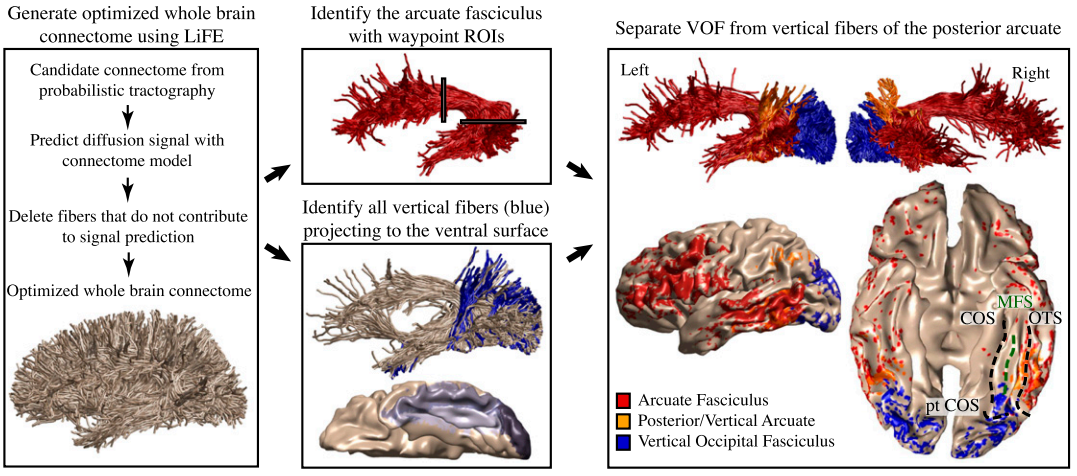

Fig. 6. Automated identification of the VOF using dMRI, T1, and tractography. Tractography is used to estimate a whole brain connectome of fiber tracts. Linear fascicle evaluation (LiFE) (51) reduces the complete set by removing fibers that are not needed to explain the diffusion signal. The arcuate fasciculus is identified from the whole-brain connectome using the waypoint region of interest (ROI) approach implemented in the automated fiber quantification (AFQ) software. FreeSurfer is used to automatically segment the cortical surface to define an ROI of ventral occipitotemporal cortex including the fusiform gyrus, inferior temporal gyrus, and lateral occipital regions (shades of gray). All of the fibers terminating within 2 mm of the ventral surface are extracted from the whole-brain connectome (beige). From this ventral occipitotemporal fiber group, all of the vertical fibers (blue) become VOF candidates. Finally, the vertical fiber group is split into vertical fibers that overlap with the arcuate fasciculus (orange) and vertical fibers that are spatially separate and posterior to the arcuate. The latter fibers are the VOF (blue). Data shown for a single, representative subject. CoS, collateral sulcus; MFS, mid-fusiform sulcus; OTS, occipitotemporal sulcus; ptCoS, posterior transverse collateral sulcus.

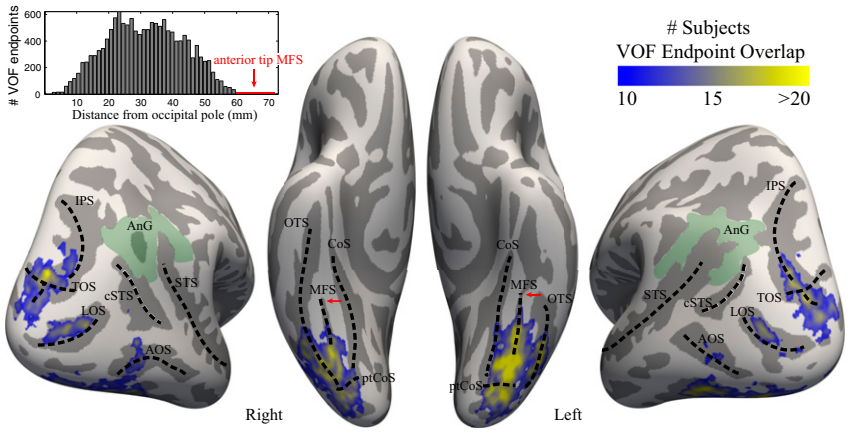

Fig. 7. The VOF terminates in consistent locations in ventral and lateral occipitotemporal cortex. VOF endpoints were projected to the cortical surface and registered to the FreeSurfer group average template. The color map shows regions of maximal VOF overlap across 37 subjects ($n = 37$). The VOF usually begins 1–1.5 cm anterior to the occipital pole and its anterior boundary is near the midpoint of the mid-fusiform sulcus (MFS). The histogram (*Upper Left*) shows the distance of each fiber's ventral termination from the occipital pole in MNI coordinates (for all subjects). The VOF rarely extends as far anterior as the anterior tip of the MFS (red arrow shows the mean MNI coordinate and SD across subjects from ref. 49). Relevant sulci and gyri are delineated with dotted black lines. AnG, angular gyrus; AOS, anterior occipital sulcus [also referred to as ascending limb of the inferior temporal sulcus (ALITS) (50) or the posterior inferior temporal sulcus (pITS) (92)]; CoS, collateral sulcus; cSTS, caudal branch of the superior temporal sulcus [also referred to as cSTS3 (50) or posterior superior temporal sulcus (pSTS) (92)]; IPS, intraparietal sulcus; LOS, lateral occipital sulcus; MFS, mid-fusiform sulcus; OTS, occipitotemporal sulcus; ptCoS, posterior transverse collateral sulcus; STS, superior temporal sulcus; TOS, transverse occipital sulcus.

cm anterior to the occipital pole. This sheet of vertical fibers spans the length of the occipital lobe and into the ventral temporal lobe. On average, the fiber tract extends 4.7 cm (SD = 0.56 cm) in the left hemisphere and 5.4 cm (SD = 0.62 cm) in the right hemisphere with an average fiber length of 3.1 cm (SD = 0.42 cm). Using the linear fascicle evaluation (LiFE) (51) software, we determined that, in every hemisphere, the existence of the VOF predicts a significant amount of the variance ($P < 0.0001$) in the measured diffusion signal.

Fig. 6 shows a rendering of the VOF and adjacent arcuate fasciculus, in both hemispheres, for a representative subject. The anterior extent of the VOF abuts the arcuate fasciculus, but these two pathways follow distinct trajectories. The posterior arcuate terminates dorsally in the parietal lobe, whereas the

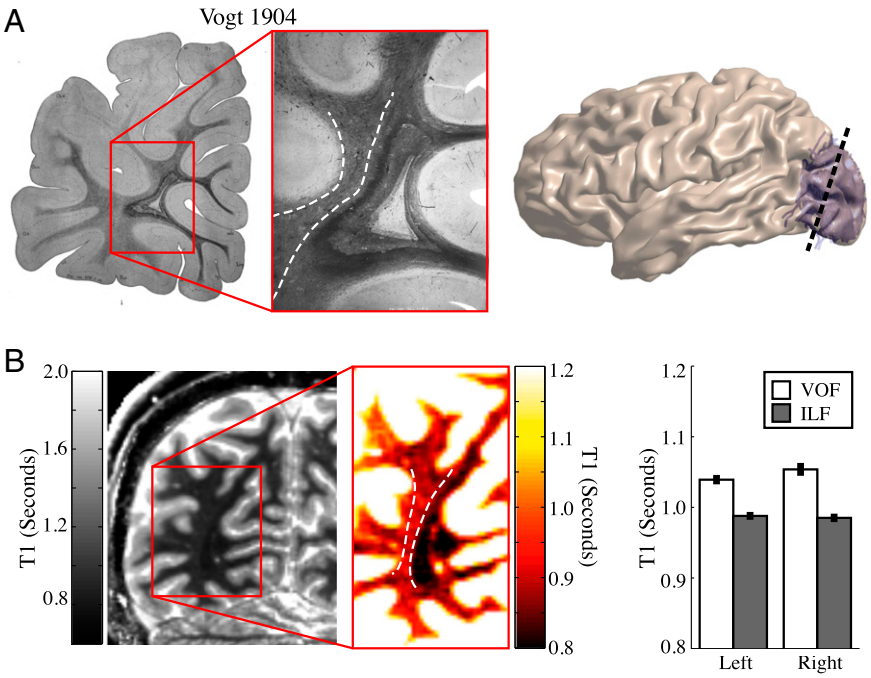

Fig. 8. The VOF can be segregated from adjacent tracts based on differences in tissue properties. (*A*) Postmortem section from Vogt (1904) (9) stained for myelin. The VOF stains lighter than nearby occipital lobe tracts, the ILF, IFOF, and optic radiations. (*B*) In vivo quantitative T1 measurements capture the same differences in occipital lobe white-matter tissue properties as the postmortem myelin stains. The expanded T1 scale for the inset shows that T1 in the VOF is higher than in the adjacent medial tracts (ILF). The difference in T1 between the VOF and ILF is present in each brain and the mean difference in T1 is highly significant ($P < 0.001$, $n = 74$) (error bars are mean ±1 SEM).

dorsal VOF is mainly confined to the occipital lobe. Few VOF fibers terminate in the angular gyrus.

Ventral VOF Terminations Divide Anterior from Posterior Ventral Occipitotemporal Cortex. The ventral VOF terminations form a stereotypical pattern with respect to the major macroanatomical features of VOT cortex (Fig. 7). There is a concentration of posterior VOF endpoints in the inferior occipital gyrus, inferior occipital sulcus, and the posterior transverse collateral sulcus. The endpoints extend in the anterior direction to the posterior mid-fusiform sulcus, lateral portions of the posterior fusiform gyrus, and posterior occipito-temporal sulcus (Fig. 7). The VOF rarely extends to the lateral branch of the collateral sulcus and never extends to the collateral sulcus proper (52).

The anterior boundary of the VOF systematically terminates near the midpoint of the mid-fusiform sulcus (MFS). The midpoint of the MFS is also a known cytoarchitectonic boundary and is thought of as dividing anterior from posterior VOT, as well as lateral from medial VOT (49). Few, if any, VOF endpoints reach the anterior tip of the MFS. By comparison, the arcuate consistently terminates in the anterior portions of the MFS and the lateral fusiform gyrus (Fig. 6).

Dorsal VOF Endpoints Project to the Transverse Occipital Sulcus and the Posterior Intraparietal Sulcus. The dorsal VOF terminations consistently fall within the transverse occipital sulcus (TOS) and posterior intraparietal sulcus (IPS) extending into the middle occipital gyrus and lateral occipital sulcus. The TOS also identifies the rostral extent of a cytoarchitectonic boundary (53). The endpoints rarely reach the three rami of the superior temporal sulcus that have recently been clarified (50). In fact, the VOF endpoints seldom reach the modern definition of the angular gyrus even though the angular gyrus was included as the superior limit of the original VOF description by Wernicke (1881) (Fig. 7). In summary, the inferior-superior fibers of the VOF span a length from ~1 cm anterior to the occipital pole to just posterior to the superior temporal sulcus.

Quantitative in Vivo Histology. The images in Sachs (1892) and Vogt (1904) reveal differences in myelination between the VOF and the neighboring inferior longitudinal fasciculus, inferior fronto-occipital fasciculus, and optic radiations (Fig. 8) (4, 9). These differences can be seen clearly despite the fact that these authors used different staining techniques. Quantitative MRI measurements can now be used to quantify the differences in tissue composition between the VOF and neighboring white-matter fascicles, in vivo.

Quantitative T1 mapping measures the longitudinal relaxation rate, with units of seconds, of water protons in a magnetic field (54). This rate depends upon at least two factors. First, the amount of tissue (macromolecules and lipid membranes) in a voxel: A voxel that is filled primarily with water will have a much higher T1 value (~4.5 s) than one that also has tissue (~1 s). Second, the type of tissue also influences the T1 value (55–58). Myelin, for example, has a particularly strong influence on the T1 value.

The VOF can be distinguished from adjacent white matter based on differences in T1 relaxation rates (Fig. 8), much as differences in myelin stain density identifies the VOF in the postmortem brain. The heavily myelinated ILF, IFOF, and optic radiations appear dark in the T1 map, whereas the VOF (dotted white outline) is much brighter. The difference in tissue properties between the VOF and adjacent white matter can be appreciated in each individual brain ($P < 0.0001$), and likely influences the nature of the signals carried by the pathway.

Discussion

Linking the VOF to Functional and Cytoarchitectonic Divisions of the Occipital Lobe. Much of modern visual neuroscience has focused on understanding functional responses in LOT and VOT cortex. This interest has been driven by the discovery of category-selective responses throughout VOT and LOT, including regions that are preferentially responsive to words (59–61), faces (62–64), body parts (48, 64, 65), places (66), and objects (67, 68).

Although it was once thought that only primary sensory areas (e.g., V1) were located in consistent anatomical locations, functional measurements projected to the cortical surface of individual brains show that regions throughout the visual hierarchy are located in predictable locations with respect to cortical folds. Just as the V1 map is reliably located in the calcarine sulcus (69, 70), MT is found in the anterior occipital sulcus (71), V3A abuts and extends into the TOS (72, 73), and the hV4 map is located in the posterior transverse collateral sulcus (74). Moreover, the fusiform face area is composed of at least two distinct regions well-predicted by the MFS (49, 63, 64), the parahippocampal place area is located within the collateral sulcus (72), and the visual word form area is reliably found in the posterior occipitotemporal sulcus (OTS) (15, 61, 75).

Cytoarchitectonic organization and white-matter connectivity likely contribute to the consistent positioning of functional regions in LOT and VOT. The MFS ventrally (49) and the TOS dorsally (53) identify cytoarchitectonic transitions. The MFS and TOS also predictably identify VOF endpoints (Figs. 6 and 7). Underlying cytoarchitectonic organization contributes to the local computational processing within a functional region. The VOF then communicates these signals between regions in the dorsal and ventral visual pathways. For example, the anterior portion of the VOF may contribute to skilled reading by linking eye movement information in the TOS/posterior IPS to word form representations in the posterior OTS (15). Furthermore, the posterior portion of the VOF connects visual field maps on the ventral (hV4) and dorsal (V3A) surface, likely communicating form and spatial orienting information between the two visual streams (76). However, the VOF is a large sheet of white matter extending 5.5 cm in length (Fig. 7). Thus, there most certainly will be additional functional subdivisions along this length linking information between the ventral and dorsal visual streams for several visual domains.

Our conclusions are based on measurements made in humans. It is not known in what species Wernicke's original observations were conducted. If the VOF does exist in macaque, the general function of the VOF—to communicate functional signals between ventral and dorsal visual cortex—might be homologous. Nevertheless, as many visual areas are not homologous across species, it is also likely that the VOF connects different functional regions in human compared with monkey. Future studies will determine the differences and similarities among species.

The Power of an Automated, Computational Definition of the VOF. Historically, anatomical results were largely communicated using example images and camera lucida drawings. The increased power of computational methods now permits investigators to develop and share algorithms that reliably define important anatomical features. There are algorithms for identifying major white-matter fascicles (77–80), parcellating the cortical surface (81, 82), and establishing cytoarchitectonic divisions in stained sections of cortex (83). In this work, we developed a reliable and automated definition of the VOF.

A computational definition of the VOF has several benefits over manual labeling methods. First, data and computational sharing assist in reproducibility. Data quality may differ between laboratories or over time, but computational methods can be standardized to eliminate variability introduced by researchers. Second, automated algorithms permit large-scale studies of VOF properties with respect to behavioral measurements and clinical symptoms. Third, computational definitions provide a clear method for expressing ideas about the rules for labeling a pathway. For example, Bartsch and colleagues confuse the posterior

arcuate with the VOF (40–42). Using computational algorithms and high-quality 3D visualization methods to define pathways can reduce such confusions. Finally, new ideas and knowledge can be incorporated into the code, capturing advances in our understanding.

The field of neuroscience was born from careful, postmortem measurements that continue to influence modern theories of brain function and are accepted by many as the gold standard, against which all future measurements should be compared. The powerful, and rapidly evolving set of neuroimaging methods that are now available have made it possible to make precise measurements of the living human brain. These in vivo techniques open an era of scalable data collection, reproducible computations, longitudinal measurements, and, for the first time (to our knowledge), the ability to test theories of human cognition in healthy, behavior participants. As the field of cognitive neuroscience evolves, it is important for researchers conducting in vivo measurements to strive for the same precision as postmortem techniques, and to develop new gold standards of in vivo measurements that are directly linked to behavior in the living human brain.

Methods

Diffusion-Weighted Imaging Data Acquisition and Preprocessing. All MRI data were collected on a General Electric Discovery 750 (General Electric Healthcare) equipped with a 32-channel head coil (Nova Medical) at the Center for Cognitive and Neurobiological Imaging at Stanford University (cni.stanford.edu). Diffusion-weighted magnetic resonance imaging (dMRI) was acquired on 37 healthy participants.

dMRI data were acquired using dual-spin echo diffusion-weighted sequences with full brain coverage. Diffusion weighting gradients were applied at 96 noncollinear directions across the surface of a sphere as determined by the electro-static repulsion algorithm (84). In all subjects, dMRI data were acquired at 2.0 mm^3 spatial resolution and diffusion gradient strength was set to b = 2,000 s/mm^2. We acquired eight non–diffusion-weighted b = 0 images at the beginning of each measurement. The full acquisition took ∼14 min.

In five subjects, an additional acquisition was acquired at high spatial resolution (1.5 mm^3). This acquisition was repeated four times and averaged to improve the signal quality. The full set of high-resolution measurements for each subject took ∼120 min.

Subjects' motion was corrected using a rigid body alignment algorithm. Diffusion gradients were adjusted to account for the rotation applied to the measurements during motion correction. The dual-spin echo sequence we used does not require performing eddy current correction because it has a relatively long delay between the radiofrequency excitation pulse and image acquisition. This allows sufficient time for the eddy currents to dephase. Preprocessing was implemented in MATLAB (MathWorks) and are publicly available as part of the vistasoft software distribution (github.com/vistalab/vistasoft/mrDiffusion; see dtiInit.m).

Fiber Tracking and Fiber Tract Segmentation. Constrained spherical deconvolution was used to estimate the fiber orientation distribution function from the diffusion signal in each voxel (lmax = 8) (85). Probabilistic tractography was used to generate a whole-brain projectome of 500,000 estimated fibers randomly seeded throughout the brain volume. LiFE was then used to determine which fiber estimates make a significant contribution to a predictive model of the diffusion signal, removing fibers that do not significantly contribute to predicting the diffusion signal (false positives) (51).

Fiber tract segmentation was performed using the AFQ software package (version 1.2). For this manuscript, additional routines were written to automatically define the VOF from the whole-brain connectome and these algorithms are distributed as open-source MATLAB code within the AFQ software package (github.com/jyeatman/AFQ/), "VOF" toolbox. For more details, see *Results* and Fig. 6.

Quantitative T1 Mapping Protocol. The quantitative T1 (1/T1) relaxation was measured from spoiled gradient echo (spoiled-GE) images acquired with different flip angles [α = 4°, 10°, 20°, 30°; repetition time (TR) = 14 ms; echo time (TE) = 2.4 ms]. The scan resolution was 1 mm^3.

The transmit coil inhomogeneity was corrected by comparing T1 measured with an additional spin echo inversion recovery (SEIR) scan (86) that is free from transmit coil inhomogeneity (86, 87). The SEIR was done with an echo-planar imaging (EPI) readout, a slab inversion pulse, and spectral spatial fat suppression. For the SEIR-EPI acquisition, the TR was 3 s; TE was set to minimum full; inversion times were 50, 400, 1,200, and 2,400 ms. We used 2 mm^2 in-plane resolution with a slice thickness of 4 mm. The EPI readout was performed using 2× acceleration to minimize spatial distortions. We used the ANTS software package to register the spoiled-GE images to match the SEIR-EPI image (88). The transmit-coil inhomogeneity was calculated by combining the unbiased SEIR T1 fits with the spoiled-GE data (7). We use the estimated transmit-coil inhomogeneity and the multi flip-angle spoiled-GE measurements to derive the T1 maps. These were calculated using a nonlinear least-squares fitting procedure to minimize the difference between the data and the spoiled-GE signal equation predictions (89). We release the T1 analysis pipeline as open-source MATLAB code (github.com/mezera/mrQ).

Three-Dimensional Mesh Construction and Visualization. All data visualization was done using the AFQ "3Dmesh" toolbox. Cortical meshes were constructed from Freesurfer segmentations of each subject's T1-weighted image (see AFQ_meshCreate.m). Each fiber has a weight associated with it that quantifies the amount of variance in the diffusion signal that is predicted by that fiber. Higher weights can be thought of as a higher volume fraction meaning that it accounts for a substantial amount of the diffusion measurements along its length. Fiber weights are mapped to the cortical surface by first computing the distance of each fiber endpoint to each mesh vertex. Then the fiber's weight is divided among nearby mesh vertices using three criteria: (*i*) only vertices within 5 mm of the fiber endpoint are considered (hard threshold); (*ii*) a fiber's weight is mapped primarily to the closest vertices, with the falloff computed as the reciprocal of the distance between the fiber endpoint and the mesh vertex; (*iii*) the units of the weights are conserved by ensuring that the values at the vertices sum to the original weight associated with the fiber. This procedure captures the inherent uncertainty of the precise cortical termination of the fiber. For more details, see AFQ_meshAddFgEndpoints.m. Cortical meshes were rendered in the MATLAB rendering environment using AFQ_RenderCorticalSurface.m.

ACKNOWLEDGMENTS. We thank Andreas Rauschecker and Bernhard Staresina for help with translations of many of the original texts. This work was funded by National Science Foundation (NSF) Grant BCS1228397 and NIH Grant EY015000 (to B.A.W.), NSF Graduate Research Fellowship (to J.D.Y.), NIH Grant 1 R01 EY 02391501 A1 (to Kalanit Grill-Spector), and NIH National Research Service Award F32 EY022294 (to A.R.).

1. Wernicke C (1881) *Lehrbuch der Gehirnkrankheiten für Ärzte und Studierende* (Verlag von Theodor Fischer, Kassel).
2. Obersteiner H (1888) *Anleitung beim Studium des Baues der Nervösen Centralorgane im Gesunden und Kranken Zustande* (Toeplitz & Deuticke, Leipzig, Germany).
3. Schnopfhagen F (1891) *Die Entstehung der Windungen des Grosshirns* (Franz Deutike, Leipzig, Germany).
4. Sachs H (1892) *Das Hemisphärenmark des Menschlichen Grosshirns. I. Der Hinterhauptlappen. Breslau. Universität. Psychiatrische und Nervenklinik*. (G. Thieme, Leipzig, Germany).
5. Schafer EA, Thane GD (1893) *Quain's Elements of Anatomy* (Bradbury, Agnew, & Co., London).
6. Vialet (1893) *Les Centres Cerebraux de la Vision et l'Appareil Nerveux Visuel Intracerebral* (Felix Alcan, Paris).
7. Barker LF (1899) *The Nervous System and Its Constituent Neurones* (D. Appelton and Company, New York).
8. Gordinier HG (1899) *The Gross and Minute Anatomy of the Central Nervous System* (P. Blakiston, Son & Company, Philadelphia).
9. Vogt O (1904) *Neurobiologische Arbeiten* (Verlag von Gustav Fischer, Jena, Germany).
10. Campbell AW (1905) *Histological Studies on the Localisation of the Cerebral Function* (Cambridge Univ Press, Cambridge, UK).
11. von Monakow C (1905) *Gehirnpathologie. I. Allgemeine Einleitung. II. Localisation. III. Gehirnblutungen* (Alfred Holder, Vienna).
12. Archambault L (1909) The inferior longitudinal bundle and the geniculo-calcarine fasciculus. A contribution to the anatomy of the tract-systems of the cerebral hemisphere. *Albany Med Ann* 30:118–143.
13. Dejerine J (1895) *Anatomie des Centres Nerveux* (Rueff, Paris).
14. Curran EJ (1909) A new association fiber tract in the cerebrum. With remarks on the fiber tract dissection method of studying the brain. *J Comp Neurol Psychol* 19:645–656.
15. Yeatman JD, Rauschecker AM, Wandell BA (2013) Anatomy of the visual word form area: Adjacent cortical circuits and long-range white matter connections. *Brain Lang* 125(2):146–155.

16. Tilney F, Riley HA (1920) *The Form and Functions of the Central Nervous System. An Introduction to the Study of Nervous Diseases* (Paul B. Hoeber, New York).
17. Bailey P, Von Bonin G, Garol HW, McCulloch WS (1943) Long association fibers in cerebral hemispheres of monkey and chimpanzee. *J Neurophysiol* 6:129–134.
18. Gray H (1918) *Anatomy of the Human Body*, ed Lewis WH (Lea & Febiger, Philadelphia).
19. Meynert T (1872) *Handbuch der Lehre von den Geweben des Menschen und der Thiere*, ed Stricker S (The New Sydenham Society, London), pp 694–808.
20. Burdach KF (1819) *Vom Baue und Leben des Gehirns* (Dyk'sche Buchhandlung, Leipzig, Germany).
21. Arnold F (1822) *Handbuch der Anatomie des Menschen* (Verlag, Freiburg, Germany).
22. Charcot JM (1883) *The Localisation of Cerebral and Spinal Diseases*, ed Hadden WB (The New Sydenham Society, London).
23. Geschwind N (1974) *Selected Papers on Language and the Brain* (Springer, New York).
24. Jakob C (1901) *Atlas of the Nervous System*, ed Fisher ED (Saunders, Philadelphia).
25. Herrick CJ (1918) *An Introduction to Neurology* (Saunders, Philadelphia).
26. Kuhlenbeck H (1927) *Vorlesungen über das Zentralnervensystem der Wirbeltiere* (Fischer, Jena, Germany).
27. Edinger L (1896) *Vorlesungen über den Bau der Nervösen Centralorgane des Menschen und der Thiere: Für Ärzte und Studierende* (F. C. W. Vogel, Leipzig, Germany).
28. Ecker A (1873) *The Cerebral Convolutions of Man*, ed Edes RT (D. Appelton and Company, New York).
29. Ecker A (1869) *Die Hirnwindung des Menschen* (Viewig, Braunschweig, Germany).
30. Ross J (1883) Reviews and notices of books—Lehrbuch der Gehirnkrankheiten für Aerzte und Studierende. Von Dr. C. Wernicke. 3 vols. Fischer, Kassel, 1881–1883. *Brain* 6(3):398–403.
31. Obersteiner H (1890) *The Anatomy of the Central Nervous Organs in Health and in Disease* (P. Blakiston, Son & Company, Philadelphia).
32. Bailey P, Von Bonin G (1951) *The Isocortex of Man* (Univ of Illinois Press, Urbana, IL).
33. Sachs B (1893) The late professor Meynert. *Am J Insa* 50(4):588–590.
34. Meynert T (1892) [Neue Studien über die Associations-Bündel des Hirnmantels]. *Indicators of the Austrian Academy of Sciences, Math-Natural Sci Class* 101(3):361–380. German.
35. Jamieson EB (1909) The means of displaying, by ordinary dissection, the larger tracts of white matter of the brain in their continuity. *J Anat Physiol* 43(3):225–234.
36. Hoeve HJH (1909) A modern method of teaching the anatomy of the brain. *Anat Rec* 3:247–253.
37. Schmahmann JD, Pandya DN (2006) *Fiber Pathways of the Brain* (Oxford Univ Press, New York).
38. Greenblatt SH (1973) Alexia without agraphia or hemianopsia. Anatomical analysis of an autopsied case. *Brain* 96(2):307–316.
39. Greenblatt SH (1976) Subangular alexia without agraphia or hemianopsia. *Brain Lang* 3(2):229–245.
40. Martino J, et al. (2013) Fiber dissection and diffusion tensor imaging tractography study of the temporoparietal fiber intersection area. *Neurosurgery* 72(1, Suppl Operative):87–97, discussion 97–98.
41. Martino J, García-Porrero JA (2013) Wernicke perpendicular fasciculus and vertical portion of the superior longitudinal fasciculus: In reply. *Neurosurgery* 73(2): E382–E383.
42. Bartsch AJ, Geletneky K, Jbabdi S (2013) The temporoparietal fiber intersection area and Wernicke perpendicular fasciculus. *Neurosurgery* 73(2):E381–E382.
43. Wernicke C (1876) Das Urwindungssystem des Menschlichen Gehirns. *Arch Psychiatr Nervenkr* 6:298–326.
44. Smith GE (1904) Studies in the morphology of the human brain with special reference to that of the Egyptians. *Rec Sch Med Egypt Gov Sch Med* 2:125–173.
45. Cunningham DJ (1892) *Contribution to the Surface Anatomy of the Cerebral Hemispheres* (Ponsonby & Weldrick, Dublin).
46. Eberstaller O (1890) *Das Stirnhirn. Ein Beitrag zur Anatomie der Oberfläche des Grosshirns* (Urban & Schwarzenberg, Vienna).
47. Homola GA, Jbabdi S, Beckmann CF, Bartsch AJ (2012) A brain network processing the age of faces. *PLoS One* 7(11):e49451.
48. Weiner KS, Grill-Spector K (2013) Neural representations of faces and limbs neighbor in human high-level visual cortex: Evidence for a new organization principle. *Psychol Res* 77(1):74–97.
49. Weiner KS, et al. (2014) The mid-fusiform sulcus: A landmark identifying both cytoarchitectonic and functional divisions of human ventral temporal cortex. *Neuroimage* 84:453–465.
50. Segal E, Petrides M (2012) The morphology and variability of the caudal rami of the superior temporal sulcus. *Eur J Neurosci* 36(1):2035–2053.
51. Pestilli F, Yeatman JD, Rokem A, Kay KN, Wandell BA (2014) Evaluation and statistical inference for human connectomes. *Nat Methods* 11(10):1058–1063.
52. Huntgeburth SC, Petrides M (2012) Morphological patterns of the collateral sulcus in the human brain. *Eur J Neurosci* 35(8):1295–1311.
53. Kujovic M, et al. (2013) Cytoarchitectonic mapping of the human dorsal extrastriate cortex. *Brain Struct Funct* 218:157–172.
54. Tofts P (2003) *Quantitative MRI of the Brain: Measuring Changes Caused by Disease* (Wiley, West Sussex, UK).
55. Bottomley PA, Foster TH, Argersinger RE, Pfeifer LM (1984) A review of normal tissue hydrogen NMR relaxation times and relaxation mechanisms from 1–100 MHz: Dependence on tissue type, NMR frequency, temperature, species, excision, and age. *Med Phys* 11(4):425–448.
56. Kucharczyk W, Macdonald PM, Stanisz GJ, Henkelman RM (1994) Relaxivity and magnetization transfer of white matter lipids at MR imaging: Importance of cerebrosides and pH. *Radiology* 192(2):521–529.
57. Mansfield P (1982) *NMR Imaging in Biomedicine: Supplement 2, Advances in Magnetic Resonance* (Academic, New York).
58. Rooney WD, et al. (2007) Magnetic field and tissue dependencies of human brain longitudinal ^1H_2O relaxation in vivo. *Magn Reson Med* 57(2):308–318.
59. Cohen L, et al. (2000) The visual word form area: Spatial and temporal characterization of an initial stage of reading in normal subjects and posterior split-brain patients. *Brain* 123(Pt 2):291–307.
60. Rauschecker AM, et al. (2011) Visual feature-tolerance in the reading network. *Neuron* 71(5):941–953.
61. Wandell BA, Rauschecker AM, Yeatman JD (2012) Learning to see words. *Annu Rev Psychol* 63:31–53.
62. Kanwisher N, McDermott J, Chun MM (1997) The fusiform face area: A module in human extrastriate cortex specialized for face perception. *J Neurosci* 17(11):4302–4311.
63. Weiner KS, Grill-Spector K (2012) The improbable simplicity of the fusiform face area. *Trends Cogn Sci* 16(5):251–254.
64. Weiner KS, Grill-Spector K (2010) Sparsely-distributed organization of face and limb activations in human ventral temporal cortex. *Neuroimage* 52(4):1559–1573.
65. Peelen MV, Downing PE (2005) Selectivity for the human body in the fusiform gyrus. *J Neurophysiol* 93(1):603–608.
66. Epstein R, Kanwisher N (1998) A cortical representation of the local visual environment. *Nature* 392(6676):598–601.
67. Grill-Spector K, Kourtzi Z, Kanwisher N (2001) The lateral occipital complex and its role in object recognition. *Vision Res* 41(10-11):1409–1422.
68. Grill-Spector K, et al. (1999) Differential processing of objects under various viewing conditions in the human lateral occipital complex. *Neuron* 24(1):187–203.
69. Inouye T (1909) *Die Sehstörungen bei Schussverletzungen der Kortikalen Sehsphäre nach Beobachtungen an Verwundeten der Letzten Japanischen Kriege* (W. Engelmann, Leipzig, Germany).
70. Henschen S (1893) On the visual path and centre. *Brain* 16:170–180.
71. Dumoulin SO, et al. (2000) A new anatomical landmark for reliable identification of human area V5/MT: A quantitative analysis of sulcal patterning. *Cereb Cortex* 10(5): 454–463.
72. Nasr S, et al. (2011) Scene-selective cortical regions in human and nonhuman primates. *J Neurosci* 31(39):13771–13785.
73. Tootell RB, et al. (1997) Functional analysis of V3A and related areas in human visual cortex. *J Neurosci* 17(18):7060–7078.
74. Witthoft N, et al. (2014) Where is human V4? Predicting the location of hV4 and VO1 from cortical folding. *Cereb Cortex* 24(9):2401–2408.
75. Ben-Shachar M, Dougherty RF, Deutsch GK, Wandell BA (2007) Differential sensitivity to words and shapes in ventral occipito-temporal cortex. *Cereb Cortex* 17(7):1604–1611.
76. Takemura H, et al. (2013) Human white matter fascicles between ventral and dorsal visual field maps. *Soc Neurosci Abstr* 39:120.02.
77. Yendiki A, et al. (2011) Automated probabilistic reconstruction of white-matter pathways in health and disease using an atlas of the underlying anatomy. *Front Neuroinform* 5:23.
78. Yeatman JD, Dougherty RF, Myall NJ, Wandell BA, Feldman HM (2012) Tract profiles of white matter properties: Automating fiber-tract quantification. *PLoS One* 7(11): e49790.
79. Wakana S, et al. (2007) Reproducibility of quantitative tractography methods applied to cerebral white matter. *Neuroimage* 36(3):630–644.
80. Wakana S, Jiang H, Nagae-Poetscher LM, van Zijl PCM, Mori S (2004) Fiber tract-based atlas of human white matter anatomy. *Radiology* 230(1):77–87.
81. Fischl B (2012) FreeSurfer. *Neuroimage* 62(2):774–781.
82. Benson NC, et al. (2012) The retinotopic organization of striate cortex is well predicted by surface topology. *Curr Biol* 22(21):2081–2085.
83. Schleicher A, Amunts K, Geyer S, Morosan P, Zilles K (1999) Observer-independent method for microstructural parcellation of cerebral cortex: A quantitative approach to cytoarchitectonics. *Neuroimage* 9(1):165–177.
84. Jones DK, Horsfield MA, Simmons A (1999) Optimal strategies for measuring diffusion in anisotropic systems by magnetic resonance imaging. *Magn Reson Med* 42(3): 515–525.
85. Tournier J-D, et al. (2008) Resolving crossing fibres using constrained spherical deconvolution: Validation using diffusion-weighted imaging phantom data. *Neuroimage* 42(2):617–625.
86. Mezer A, et al. (2013) Quantifying the local tissue volume and composition in individual brains with MRI. *Nat Med* 19(12):1667–1672.
87. Barral JK, et al. (2010) A robust methodology for in vivo T1 mapping. *Magn Reson Med* 64(4):1057–1067.
88. Avants B, Gee JC (2004) Geodesic estimation for large deformation anatomical shape averaging and interpolation. *Neuroimage* 23(Suppl 1):S139–S150.
89. Chang L-C, Koay CG, Basser PJ, Pierpaoli C (2008) Linear least-squares method for unbiased estimation of T1 from SPGR signals. *Magn Reson Med* 60(2):496–501.
90. Edinger L (1885) *Zehn Vorlesungen über den Bau der Nervösen Centralorgane. Für Ärzte und Studierende* (F. C. W. Vogel, Leipzig, Germany).
91. Edinger L (1904) *Vorlesungen über den Bau der Nervösen Centralorgane des Menschen und der Thiere: Für Ärzte und Studierende* (F.C.W. Vogel, Leipzig, Germany).
92. Weiner KS, Grill-Spector K (2011) Not one extrastriate body area: Using anatomical landmarks, hMT+, and visual field maps to parcellate limb-selective activations in human lateral occipitotemporal cortex. *Neuroimage* 56(4):2183–2199.